

Search for light bosonic dark matter in a side-band analysis of a ^{199}Hg free-spin precession signal

P. Schmidt-Wellenburg^{1,*} and A. Author²

¹*Paul Scherrer Institut, CH-5232 Villigen PSI, Switzerland*

²*An institute, somewhere*

Abstract

Ultra low mass bosons are viable dark matter candidates and may form a coherent oscillation background field. Nuclear spins in experiments on Earth couple to this oscillating dark matter field, when propagating on the Earth trajectory through our galaxy. This coupling to the spin can be thought of as oscillating pseudo-magnetic field which modulates the spin precession of the nuclear spin. Here we report on the null result of an experiment searching for a frequency modulation of the free spin-precession signal of ^{199}Hg in a 1038 nT magnetic field.

Keywords: dark matter, axion, axion-like-particle, beyond Standard Model physics, magnetic resonance spectroscopy

Introduction

The existence of cold dark matter (DM) is a cornerstone of the cosmological standard model [1], while the standard model of particle physics (SM) [2] convincingly describes all laboratory known fundamental constituents of matter and their interaction. The discovery of the microscopic constituents and fundamental interactions of DM, which makes up 80% of the matter content of the Universe, and how it fits into the SM would resolve one of the most intriguing riddles of modern science.

One very well motivated category of candidates for cold DM is the class of axion-like particles (ALP). The prototype of these pseudoscalar bosons, the canonical axion, was first introduced by Peccei and Quinn [3] to resolve the strong CP-problem in quantum chromodynamics (QCD) [4–7]. More generic axion-like particles are spin-0 bosons where the stringent relation between coupling and mass to match the QCD CP-problem are relaxed. These ALPs and other ultra low mass bosons are common to many beyond SM theories and naturally provide a sufficient abundance to match the observed DM abundance [8–12]. In the remainder of this article we will follow the general taxonomy and call these DM candidates axions.

The wide range of testable parameters and the ubiquitous theoretical motivation of axions coupling to SM particles instigated a large variety of experimental searches [13–21] in the last decade. These searches exploit three possible non-gravitational interaction which lead to distinctive phenomena: coupling to photons, e.g., in searches for axions coupling to microwave cavities [14, 22], emission by the sun [23], or light-shining-through-a-wall experiments [24]; coupling to gluons provoking an oscillating electric dipole moment [15, 25]; and the coupling to the spin of fermions, also known as axion-wind effect, resulting in pseudo-magnetic spin precession of fermions [16, 18, 21].

In this article we present the result from a search for the axion-wind effect exploiting the spin precession of polarized ^{199}Hg in a low magnetic field of $B = 1038\text{ nT}$, using the same apparatus as in the search for a gluonic coupling to the neutron [15]. The axion-wind search and result is based on the assumption, that our Earth passes through DM with the galactic virial velocity of $\vec{v} \approx 1 \times 10^{-3}c$, where c is the speed of light in vacuum. If the mass of the DM is below $m_{\text{DM}} \leq 10\text{ eV}/c^2$ and dominantly consists only of one type of particle the local particle density must be so high that it needs to be bosonic in nature with a large mode occupation number for an average local DM density of $\rho_{\text{DM}} = 0.4\text{ GeV}/\text{cm}^3$ to $0.8\text{ GeV}/\text{cm}^3$ [26]. In this

hypothesis the DM made of axions of mass m_a can be described as a classical field

$$a(t) = a_0 \sin(\omega_a t), \quad (1)$$

where a_0 is the amplitude oscillating at the Compton wavelength $\omega_a = m_a c^2 / \hbar$ and \hbar is the reduced Planck constant. The amplitude itself,

$$a_0 = \frac{c}{\omega_a} \sqrt{2\rho_{\text{DM}}}, \quad (2)$$

is connected to the average local DM density for which we take the lower bound of $\rho_{\text{DM}} = 0.4 \text{ GeV}/\text{cm}^3$ of the above indicated 2σ range. The characteristic coherence time of the axion field is $\tau_c = (2\pi)c^2/(v^2\omega_a) \geq T$, where T is the total measurement time.

The interaction of the axion with fermions is described by the Lagrangian [17]

$$\mathcal{L}_a = g_{a\bar{\psi}\psi} \partial_\mu a \bar{\psi} \gamma^\mu \gamma^5 \psi, \quad (3)$$

where ψ is the fermion field, e.g. the ^{199}Hg -nucleus, and $g_{a\bar{\psi}\psi}$ the coupling constant between the axion field $a(t)$ and the fermion. In our case for ^{199}Hg spin-1/2 this interaction can be expressed by the non-relativistic Hamiltonian

$$H_a = -\hbar g_{\text{aNN}} \vec{\sigma} \cdot \vec{D}, \quad (4)$$

describing the coupling of the spin to the dark matter field. In analogy to the Larmor precession this leads to a precession of the nuclear spin in the pseudomagnetic field \vec{D} where the gyromagnetic ratio γ_{Hg} is substituted by the coupling g_{aNN} .

The ^{199}Hg magnetometer measures the magnetic field B by observing the precession frequency $\omega_{\text{Hg}} = \gamma_{\text{Hg}} B$, the Larmor frequency, of the nuclear spin using the orientation dependent absorption of resonant circular light. The intensity $I_1(t)$ of resonant, circular polarized, laser light after transmission through polarized ^{199}Hg -vapor as function of time, t , can be described as

$$I_1(t)/I = e^{-\mathcal{O}_{\text{Hg}}(t)(1-P(t)\sin(\omega_{\text{Hg}}t+\phi))}, \quad (5)$$

where I is the initial light intensity, $\mathcal{O}_{\text{Hg}}(t) = n(t)\sigma_{\text{Hg}}\ell$ is the opacity of the vapor depending on the vapor density $n(t)$, the light absorption cross section σ_{Hg} , and length ℓ of the light path. The vapor polarization, $P(t) = P_0 \exp(-\Gamma_2 t)$, is a function of the initial polarization P_0 and transverse coherence time $T_2 = 1/\Gamma_2$. The vapor density $n(t) = n_0 \exp(-\Gamma_\ell t)$ decreases

with time due to the chamber specific leakage rate Γ_l , a result of mechanical imperfections. For now we ignore the effect of depolarization and vapor leakage, which in practice result in a broadening of the resonant frequency. Hence, in the presence of an oscillating axion field we will observe a frequency modulated light intensity [27]

$$I_1(t) = I_0 \cos \left(\gamma_{\text{Hg}} B t + \frac{1}{2} \int_0^t g_{\text{aNN}} v \sqrt{2\rho_{\text{DM}}} \sin(\omega_a t') dt' \right), \quad (6)$$

where I_0 is the oscillation amplitude. For a weak modulation this can be reduced to a superposition of three amplitude oscillations

$$I_1(t) \approx I_0 \left[\cos(\gamma_{\text{Hg}} B t) + \frac{g_{\text{aNN}} v \sqrt{2\rho_{\text{DM}}}}{2\omega_a} \cdot [\sin((\gamma_{\text{Hg}} B + \omega_a)t + \phi_+) + \sin((\gamma_{\text{Hg}} B - \omega_a)t + \phi_-)] \right], \quad (7)$$

using a series expansion to first order in Bessel functions of the first kind. In the frequency domain, this results in a peak with amplitude I_0 and two side-band peaks of amplitude $I_0 g_{\text{aNN}} v \sqrt{2\rho_{\text{DM}}} / (2\omega_a)$. For axion masses with oscillation frequencies $m_a c^2 / h = \omega_a < \omega_{\text{Hg}}$, we expect two narrow lines at $\omega_{2p} = \omega_{\text{Hg}} \pm \omega_a$ while for $\omega_a > \omega_{\text{Hg}}$ we search for two lines at $\omega_{2p} = \omega_a \pm \omega_{\text{Hg}}$.

Experiment setup

The measurements were performed in 2017 using the same instrument which was used for data-taking for the most sensitive measurement of the static electric dipole moment (EDM) of the neutron [28]. Figure 1 shows a sketch of the apparatus. The mercury isotope ^{199}Hg was used to measure the Larmor precession frequency $f_{\text{Hg}} = \gamma_{\text{Hg}} \langle B \rangle$, where $\gamma_{\text{Hg}} = 7.590\,115\,2(62) \text{ MHz/T}$ [29] is the gyromagnetic ratio of ^{199}Hg and $\langle B \rangle$ is the volume average magnetic field within the precession chamber. The cylindrical precession chamber of height $h = 120 \text{ mm}$ and radius $r = 235 \text{ mm}$ was made of diamond-like-carbon coated [30] aluminum top and bottom plates and an insulator ring made from polystyrene coated with deuterated polystyrene [31]. Two circular windows of about 50 mm diameter inside the insulator ring were made of quartz glass coated with deuterated polyethylene [31] and were used to shine a laser beam through the chamber to detect the precession signal. A detailed description of the mercury magnetometer and its laser upgrade can be found in refs. [32–34]. Polarized mercury was prepared inside a cylindrical volume of 1 liter just below the bottom

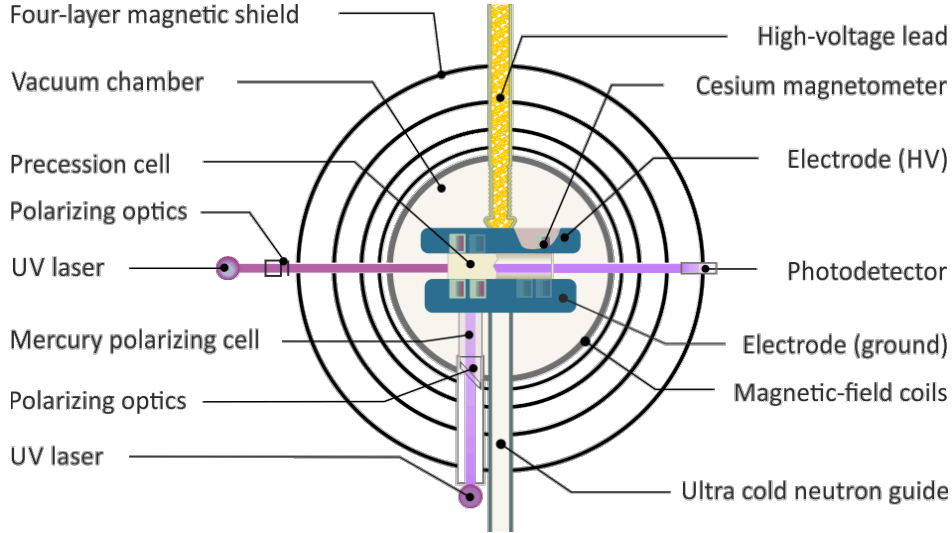


Figure 1: Sketch of the single chamber nEDM spectrometer used for the measurement and omitting details relevant only for measurements with ultracold neutrons.

plate. A shutter with 12 mm open diameter separated the volume for optical pumping, also known as polarizing chamber, from the larger volume of the precession chamber. A single measurement, also known as cycle, consisted of the following steps: the shutter between polarizing and precession chamber opened for $t = 2$ s to admit polarized ^{199}Hg vapor into the detection volume. Next, an optimized circular rotating magnetic field B_{rf} was applied during $t_{\text{rf}} = 2$ s using two split coils perpendicular to each other and perpendicular to the magnetic field B with frequency $f_{\text{rf}} = \gamma_{\text{Hg}}\langle B \rangle \approx 7.88$ Hz. The coils were wound onto the vacuum tank made of aluminum. The currents I_i generating $B_{\text{rf}}(I_i)$ were adjusted such that $\gamma_{\text{Hg}}B_{\text{rf}}(I_i)t_{\text{rf}} = \pi/2$ tilting the spin into the plane perpendicular to the magnetic field B . While one batch of polarized mercury was prepared by optical pumping [34] the other was precessing inside the precession chamber. The spin dependent light absorption of the ^{199}Hg nuclei results in an intensity modulation, proportional to the Larmor frequency, ω_{Hg} , of the circular polarized readout laser light.

The light intensity of the read out beam was recorded using a photo multiplier (PM). The signal from the PM was digitized using a 24-bit $\Delta\Sigma$ analog-to-digital converter (ADC) at a sampling frequency of 51.2 kHz of the of NI PXI-4461[?] module. The data was down-sampled to 100 Hz using a spline interpolation before it was saved to disc with an absolute time stamp of 1 ms precision. The precise timing of spin-flip pulses and ADC-sampling was controlled by an atomic clock with a relative precision of 1×10^{-12} .

Data analysis

A total of 297 free spin-precession (FSP) signals were recorded in a little more than $T = 13$ hours. Each FSP is a time series of 10000 data points recorded with a frequency of 100 Hz and a duration of $\mathcal{T} = 100$ s. In order to estimate the light intensity, I , opacity O , and polarization $P = (P_1^2 + P_2^2)^{1/2}$, we fitted the FSP time series to the first two lines of the modified equation (5),

$$I_1(t) = I \exp \left[-\mathcal{O} \exp(-\Gamma_\ell t) \right. \\ \left. + \mathcal{O} \exp(-(\Gamma_\ell + \Gamma_2)t) (P_1 \sin(\omega_{\text{Hg}} t) + P_2 \cos(\omega_{\text{Hg}} t)) \right. \quad (8)$$

$$\left. + \mathcal{O} \exp(-(\Gamma_\ell + \Gamma_2 + \Gamma_{\text{NL}})t) (P_3 \sin(2\omega_{\text{Hg}} t) + P_4 \cos(2\omega_{\text{Hg}} t)) \right]. \quad (9)$$

where $T_\ell = 1/\Gamma_\ell$ is the leakage time constant, and $T_2 = 1/\Gamma_2$ the transverse spin decoherence time. In a second step we also included the second harmonic, which appears due to non-linear effects in the detection scheme. While we kept I and O fixed to the values obtained in the first optimization, we introduced the additional parameters Γ_{NL} and $P_{\text{NL}} = (P_3^2 + P_4^2)^{1/2}$ for the second harmonic. The results of all fitted parameters are shown for the entire dataset in Figure 2. The remaining residual times series,

$$R(t) = \mathcal{N}(t) + I_0 \mathcal{O}_{\text{Hg}} e^{-(\Gamma_\ell + \Gamma_2)t} \frac{g_{\text{aNNV}} \sqrt{2\rho_{\text{DM}}}}{2\omega_a} \cdot [\sin((\gamma_{\text{Hg}} B + \omega_a)t + \phi_+) + \sin((\gamma_{\text{Hg}} B - \omega_a)t + \phi_-)], \quad (10)$$

consists of the noise $\mathcal{N}(t)$ and the hypothetical frequency modulation at ω_a . An axion background field would result in two coherent modulations of the FSP across all time-series for frequencies $\omega_a/(2\pi) = f_a < 1 \times 10^6/T \approx 21.4$ Hz. The residuals of all 297 cycles were stitched together to one long time-series using the timestamps of the atomic clock. This macro time-series was then used for a Lomb-Scargle frequency analysis [35, 36], which is ideally suited for a frequency analysis of non-equally spaced data. We average the power spectral density with an original frequency resolution of $\delta f = 1/(4T) = 5.3 \times 10^{-6}$ Hz over frequency bins equal to the $1/\mathcal{T} = 0.01$ Hz. A no signal background hypothesis is constructed by assuming only one single axion field. Hence, the measured noise floor in the direct vicinity of a peak represent the expected background in this frequency range. The noise floor, B_i , is estimated by removing up to three peak-like features per 1 Hz range using a peak finding algorithm [?] and then taking a moving average over a 500 mHz range, $B_i = \langle \mathcal{B} \rangle_{500}$. To

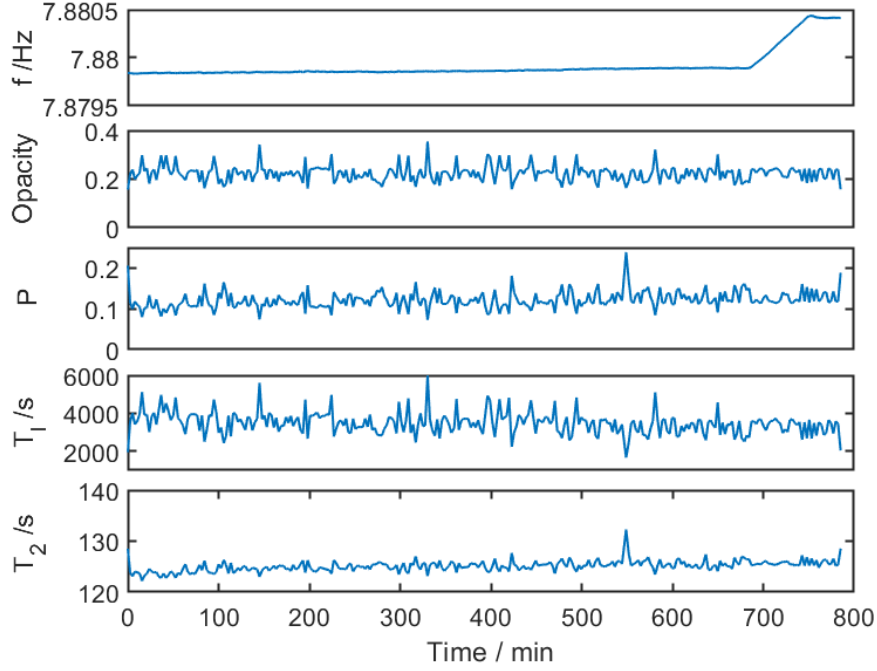


Figure 2: Results from fit of equation (9) to all FSP signals versus time in minutes. Plots show from top to bottom: the mercury Larmor frequency, f_{Hg} , the initial opacity O , the spin polarization P , the leakage time constant T_ℓ , and the transverse decoherence time constant T_2 . Note, that extracted Larmor frequencies are all well within 1 mHz, although the ramp of a strong dipole magnet in the near vicinity of the experiment is visible at times larger 660 min.

calculate the local p -value for the power $\mathcal{P}(f_i)$ of the i th frequency we take advantage of the fact that the cumulative distribution function of a white noise power spectrum follows an exponential distribution, hence

$$p_{\text{local}}(f_i) = \exp(-\mathcal{P}(f_i)/\langle B_i \rangle). \quad (11)$$

Figure 3 shows the Lomb-Scargle frequency analysis of the residuals with the 95% confidence level from the single axion hypothesis assuming the presence of two peaks. At frequencies above 32.24 Hz only one of two peaks would be detectable. Hence, 95% confidence level increases. However, for the axion search we only consider data below the inverse of the theoretical axion coherence time ω_a . We assume that the local p -values at different trial frequencies are uncorrelated and therefore calculate the global p -value by [37]

$$p_{\text{global}} = 1 - (1 - p_{\text{local}})^n, \quad (12)$$

where n is the number of trial frequencies. This results in the indicated false alarm thresholds for $2 \dots 5\sigma$ significance as green lines in fig. 3.

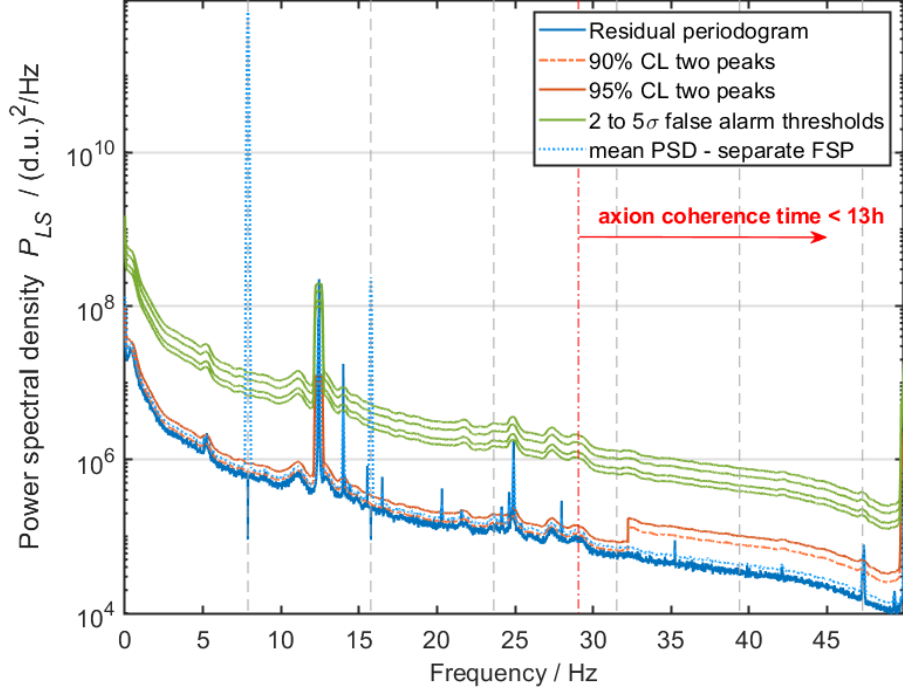


Figure 3: Lomb-Scargel power spectral density [35, 36] of fit residuals. The 95% confidence level is calculated for a two peak signal assumption. False alarm thresholds, 2σ to 5σ , are indicated for a single axion-frequency assumption. The light blue dotted line indicates the power spectral density of the averaged 297 FSPs before removing the carrier frequency. A full list of all peaks above threshold is listed in table I. The dashed vertical lines at multiples of 7.88 Hz indicate the position of the mercury Larmor frequency and higher orders. The red, dash-dotted line indicates the frequency above which the theoretical coherence time of an axion field is shorter than our measurement time.

frequency (Hz)	evidence (σ)	comment
12.45	5.8	no peak at 3.31 Hz / no peak at 28.21 Hz
13.99	10.2	no peak at 1.77 Hz / no peak at 29.76 Hz

Table I: Table of peaks above 2σ -false alarm threshold. The evidence of the peak is noted relative to the 1σ false alarm level. A coherent background field from a ultralight axion with the frequency $f_a = m/h$ would result in a frequency modulation of the carrier frequency $f_{\text{Hg}} = 7.879(1)$ Hz and would be visible as two peaks with equal power, at either $f_{\text{Hg}} \pm f_a \forall f_a < f_{\text{Hg}}$ and $f_a \pm f_{\text{Hg}}$ otherwise.

Result and Discussion

Only two peaks, at 12.45 Hz and 13.99 Hz, pass the two sigma false alarm threshold, both are missing a corresponding second peak at 3.31 Hz and 1.77 Hz or 28.21 Hz and 29.76 Hz required for a frequency modulated signal described by equation (10). Further, the peak at 12.45 Hz was also present in background data [34]. Hence, no signal was observed and we translate the Lomb-Scargel periodogram into a 95% confidence limit on the coupling constant $g_{a\text{NN}}$, between the axion field and the ^{199}Hg nucleus by calculating

$$g_{\text{aNN},95\%}(f_a) = A_{\text{osc},95\%}(f_i) \frac{4\pi(f_i - f_{\text{Hg}})}{v\sqrt{2\rho_{\text{DM}}\langle I_0 \rangle} \exp(-100/\langle \tau \rangle)}, \quad (13)$$

where $f_a = f_i - f_{\text{Hg}}$ is the trial axion frequency, $\langle \tau \rangle = \langle \Gamma_l + \Gamma_2 \rangle^{-1} = 121.5(5)$ s the mean decay time constant of the mercury precession signal with mean frequency $f_{\text{Hg}} = 7.879(1)$ Hz and mean initial oscillation amplitude $\langle I_0 \rangle$, averaged over all cycles. The oscillation amplitude, $A_{\text{osc}, 95\%}$, is calculated for a coherent signal from the 95% confidence band with

$$A_{\text{osc}, 95\%} = \sqrt{\frac{2\mathcal{P}_{95\%}}{N}}, \quad (14)$$

where N the total number of samples.

Our result for a search of axion like particle coupling to ^{199}Hg nucleons is shown in Figure 4. The insensitive regions at multiples of the carrier frequency $f_{\text{Hg}} = 7.879(1)$ Hz are not depicted. The red shaded area, labeled “PSI-HgM-sideband”, indicates the upper bound of an axion coupling to nuclear spin at the 95% confidence level in the examined frequency range. The sensitivity represents 297 free spin decay signal of 100 s duration in a magnetic field of $B = 1038$ nT taken within 13 hours of operation. Systematic effects due to the readout scheme, e.g., the real-light-shift systematic discussed in Ref.[28], are tiny with the respect to the resolution and would only change the absolute value of the carrier frequency.

Using the new double chamber neutron EDM apparatus [38] currently being setup at PSI will permit an increase in sensitivity by about a factor ten by prolonging the free precession time to 240 s, two time the coherence time, and canceling and hence reducing the intrinsic noise by using a differential detection scheme. Further, two precession chambers set one above the others each with a three times larger volume will increase the sensitivity by about a factor four alone. A change of the absolute value of the magnetic field will be used to shift the carrier frequency and hence the sideband spectra to cover the blind spots of this analysis. We will demonstrate the sensitivity of the future apparatus to axion-wind-like frequency modulations by applying frequency modulations of the magnetic field.

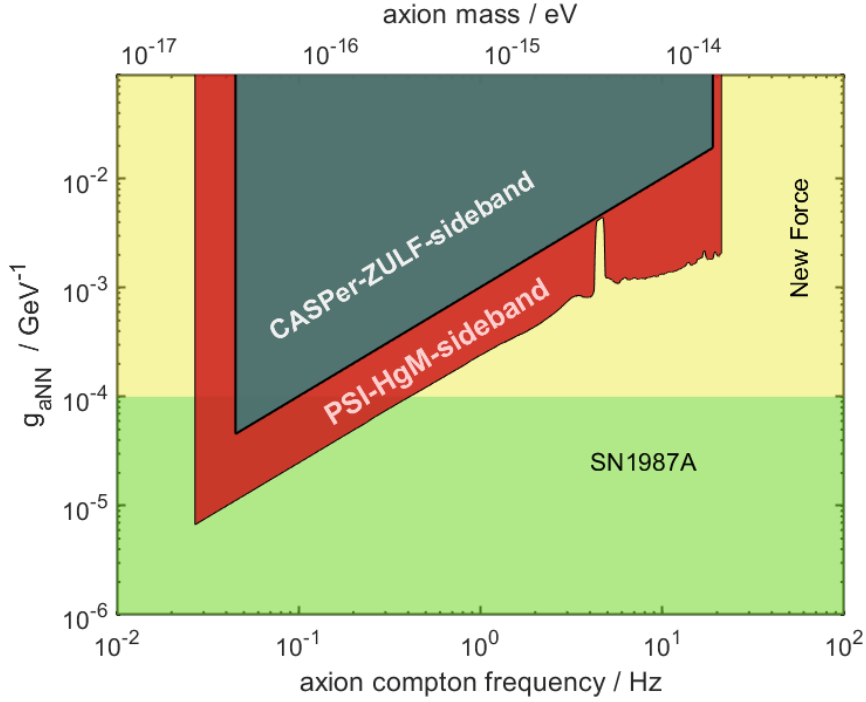


Figure 4: Exclusion plot for axion wind linear coupling g_{aNN} versus Compton frequency of the classical axion field, where $f_a = m_a/h$. The area excluded by the presented ^{199}Hg -sideband analysis at PSI with a 90% CL supersedes entirely the previous work by CASPer-ZULF [16]. The “new force” region is a limit from a search for long range spin-dependent force [39], while the area marked “SN1987A” represents existing limits from the cooling of a supernova [40].

Acknowledgments

We acknowledge the excellent support provided by the PSI technical groups and by various services of the collaborating universities and research laboratories. In particular we acknowledge with gratitude the long term outstanding technical support by F. Burri and M. Meier. We thank the UCN source operation group BSQ for their support. We acknowledge financial support from the Swiss National Science Foundation through projects No.117696, No.137664, No.144473, No.157079, No.172626, No.126562, No.169596 (all PSI), No.162574 (ETH) No.172639 (ETH).

* Corresponding author: philipp.schmidt-wellenburg@psi.ch

- [1] M. Bartelmann. ‘The Dark Universe.’ *Rev. Mod. Phys.*, 82(2010) 331. URL <http://dx.doi.org/10.1103/RevModPhys.82.331>. 0906.5036.
- [2] P. A. Zyla, R. M. Barnett, J. Beringer, *et al.* ‘Review of Particle Physics.’ *Progress of Theoretical and Experimental Physics*, 2020(2020) 083C01. URL <http://dx.doi.org/10.1093/ptep/ptaa104>.

- [3] R. D. Peccei and H. R. Quinn. ‘CP Conservation in the Presence of Pseudoparticles.’ *Phys. Rev. Lett.*, 38(1977) 1440.
- [4] S. Weinberg. ‘A New Light Boson?’ *Phys. Rev. Lett.*, 40(1978) 223. URL <http://dx.doi.org/10.1103/PhysRevLett.40.223>.
- [5] F. Wilczek. ‘Problem of Strong p and t Invariance in the Presence of Instantons.’ *Phys. Rev. Lett.*, 40(1978) 279. URL <http://dx.doi.org/10.1103/PhysRevLett.40.279>.
- [6] M. Dine, W. Fischler, and M. Srednicki. ‘A simple solution to the strong CP problem with a harmless axion.’ *Physics Letters B*, 104(1981) 199. URL [http://dx.doi.org/10.1016/0370-2693\(81\)90590-6](http://dx.doi.org/10.1016/0370-2693(81)90590-6).
- [7] J. E. Kim and G. Carosi. ‘Axions and the strong CP problem.’ *Rev. Mod. Phys.*, 82(2010) 557. URL <http://dx.doi.org/10.1103/RevModPhys.82.557>.
- [8] J. Preskill, M. B. Wise, and F. Wilczek. ‘Cosmology of the invisible axion.’ *Physics Letters B*, 120(1983) 127. URL [http://dx.doi.org/10.1016/0370-2693\(83\)90637-8](http://dx.doi.org/10.1016/0370-2693(83)90637-8).
- [9] P. Svrcak. ‘Cosmological Constant and Axions in String Theory.’ *arXiv e-prints*, (2006) hep-th/0607086. URL <https://ui.adsabs.harvard.edu/abs/2006hep.th....7086S>. hep-th/0607086.
- [10] A. Arvanitaki, S. Dimopoulos, S. Dubovsky, *et al.* ‘String axiverse.’ *Phys. Rev. D*, 81(2010) 123530. URL <http://dx.doi.org/10.1103/PhysRevD.81.123530>.
- [11] P. Arias, D. Cadamuro, M. Goodsell, *et al.* ‘WISPy cold dark matter.’ *J. Cosmology Astropart. Phys.*, 2012(2012) 013. URL <http://dx.doi.org/10.1088/1475-7516/2012/06/013>. 1201.5902.
- [12] P. W. Graham, D. E. Kaplan, and S. Rajendran. ‘Cosmological Relaxation of the Electroweak Scale.’ *Phys. Rev. Lett.*, 115(2015) 221801. URL <http://dx.doi.org/10.1103/PhysRevLett.115.221801>. 1504.07551.
- [13] D. Budker, P. W. Graham, M. Ledbetter, *et al.* ‘Proposal for a Cosmic Axion Spin Precession Experiment (CASPEr).’ *Phys. Rev.*, X4(2014) 021030. URL <http://dx.doi.org/10.1103/PhysRevX.4.021030>. 1306.6089.
- [14] B. M. Brubaker, L. Zhong, Y. V. Gurevich, *et al.* ‘First Results from a Microwave Cavity Axion Search at $24\ \mu\text{eV}$.’ *Phys. Rev. Lett.*, 118(2017) 061302. URL <http://dx.doi.org/10.1103/PhysRevLett.118.061302>. 1610.02580.
- [15] C. Abel, N. J. Ayres, G. Ban, *et al.* ‘Search for Axionlike Dark Matter through Nuclear Spin Precession in Electric and Magnetic Fields.’ *Phys. Rev. X*, 7(2017) 041034. URL <http://dx.doi.org/10.1103/PhysRevX.7.041034>.

- [16] A. Garcon, J. W. Blanchard, G. P. Centers, *et al.* ‘Constraints on bosonic dark matter from ultralow-field nuclear magnetic resonance.’ *Science Advances*, 5(2019) eaax4539. URL <http://dx.doi.org/10.1126/sciadv.aax4539>. 1902.04644.
- [17] P. W. Graham, D. E. Kaplan, J. Mardon, *et al.* ‘Spin precession experiments for light axionic dark matter.’ *Phys. Rev. D*, 97(2018) 055006. URL <http://dx.doi.org/10.1103/PhysRevD.97.055006>. 1709.07852.
- [18] T. Wu, J. W. Blanchard, G. P. Centers, *et al.* ‘Search for Axionlike Dark Matter with a Liquid-State Nuclear Spin Comagnetometer.’ *Phys. Rev. Lett.*, 122(2019) 191302. URL <http://dx.doi.org/10.1103/PhysRevLett.122.191302>.
- [19] K. M. Backes, D. A. Palken, S. A. Kenany, *et al.* ‘A quantum enhanced search for dark matter axions.’ *Nature*, 590(2021) 238. URL <http://dx.doi.org/10.1038/s41586-021-03226-7>. 2008.01853.
- [20] P. W. Graham, S. Hacıömeroğlu, D. E. Kaplan, *et al.* ‘Storage ring probes of dark matter and dark energy.’ *Phys. Rev. D*, 103(2021) 055010. URL <http://dx.doi.org/10.1103/PhysRevD.103.055010>. 2005.11867.
- [21] D. Aybas, J. Adam, E. Blumenthal, *et al.* ‘Search for Axionlike Dark Matter Using Solid-State Nuclear Magnetic Resonance.’ *Phys. Rev. Lett.*, 126(2021) 141802. URL <http://dx.doi.org/10.1103/PhysRevLett.126.141802>. 2101.01241.
- [22] J. L. Ouellet, C. P. Salemi, J. W. Foster, *et al.* ‘First Results from ABRACADABRA-10 cm: A Search for Sub- μ eV Axion Dark Matter.’ *Phys. Rev. Lett.*, 122(2019) 121802. URL <http://dx.doi.org/10.1103/PhysRevLett.122.121802>. 1810.12257.
- [23] V. Anastassopoulos, S. Aune, K. Barth, *et al.* ‘New CAST limit on the axion-photon interaction.’ *Nature Physics*, 13(2017) 584. URL <http://dx.doi.org/10.1038/nphys4109>. 1705.02290.
- [24] R. Ballou, G. Deferne, M. Finger, *et al.* ‘New exclusion limits on scalar and pseudoscalar axionlike particles from light shining through a wall.’ *Phys. Rev. D*, 92(2015) 092002. URL <http://dx.doi.org/10.1103/PhysRevD.92.092002>. 1506.08082.
- [25] T. S. Roussy, D. A. Palken, W. B. Cairncross, *et al.* ‘Experimental Constraint on Axionlike Particles over Seven Orders of Magnitude in Mass.’ *Phys. Rev. Lett.*, 126(2021) 171301. URL <http://dx.doi.org/10.1103/PhysRevLett.126.171301>.
- [26] M. Benito, F. Iocco, and A. Cuoco. ‘Uncertainties in the Galactic Dark Matter distribution: An update.’ *Physics of the Dark Universe*, 32(2021) 100826. URL <http://dx.doi.org/10.1016/j.dark.2021.100826>. 2009.13523.

- [27] P. W. Graham and S. Rajendran. ‘New Observables for Direct Detection of Axion Dark Matter.’ *Phys. Rev.*, D88(2013) 035023. URL <http://dx.doi.org/10.1103/PhysRevD.88.035023>. 1306.6088.
- [28] C. Abel, S. Afach, N. J. Ayres, *et al.* ‘Measurement of the Permanent Electric Dipole Moment of the Neutron.’ *Phys. Rev. Lett.*, 124(2020) 081803. URL <http://dx.doi.org/10.1103/PhysRevLett.124.081803>.
- [29] S. Afach, C. Baker, G. Ban, *et al.* ‘A measurement of the neutron to ^{199}Hg magnetic moment ratio.’ *Phys. Lett. B*, 739(2014) 128 .
- [30] F. Atchison, T. Brys, M. Daum, *et al.* ‘First storage of ultracold neutrons using foils coated with diamond-like carbon.’ *Phys. Lett. B*, 625(2005) 19.
- [31] K. Bodek, M. Daum, R. Henneck, *et al.* ‘Storage of ultracold neutrons in high resistivity, non-magnetic materials with high Fermi potential.’ *Nucl. Instrum. Methods A*, 597(2008) 222.
- [32] K. Green, P. G. Harris, P. Iaydjiev, *et al.* ‘Performance of an atomic mercury magnetometer in the neutron EDM experiment.’ *Nucl. Instr. Meth. Phys. Res. A*, 404(1998) 381.
- [33] G. Ban, G. Bison, K. Bodek, *et al.* ‘Demonstration of sensitivity increase in mercury free-spin-precession magnetometers due to laser-based readout for neutron electric dipole moment searches.’ *Nucl. Instr. Meth. Phys. Res. A*, 896(2018) 129. URL <http://dx.doi.org/10.1016/j.nima.2018.04.025>. 1804.05838.
- [34] S. Komposch. Realization of a high-performance laser-based mercury magnetometer for neutron EDM experiments. DISS. ETH NR. 24326, ETH Zürich (2017).
- [35] N. R. Lomb. ‘Least-Squares Frequency Analysis of Unequally Spaced Data.’ *Ap&SS*, 39(1976) 447. URL <http://dx.doi.org/10.1007/BF00648343>.
- [36] J. D. Scargle. ‘Studies in astronomical time series analysis. II. Statistical aspects of spectral analysis of unevenly spaced data.’ *ApJ*, 263(1982) 835. URL <http://dx.doi.org/10.1086/160554>.
- [37] S. Algeri, D. van Dyk, J. Conrad, and B. Anderson. ‘On methods for correcting for the look-elsewhere effect in searches for new physics.’ 11(2016) P12010. URL <http://dx.doi.org/10.1088/1748-0221/11/12/p12010>.
- [38] N. J. Ayres, G. Ban, L. Bienstman, *et al.* ‘The design of the n2EDM experiment.’ *arXiv e-prints*, (2021) arXiv:2101.08730. URL <https://ui.adsabs.harvard.edu/abs/2021arXiv210108730A>. 2101.08730.
- [39] G. Vasilakis, J. M. Brown, T. W. Kornack, and M. V. Romalis. ‘Limits on new long range nuclear spin-dependent forces set with a K - He-3 co-magnetometer.’ *Phys. Rev. Lett.*, 103(2009)

261801. URL <http://dx.doi.org/10.1103/PhysRevLett.103.261801>. 0809.4700.

[40] G. G. Raffelt. Axions: Theory, Cosmology, and Experimental Searches, 51–71. Springer, Berlin (2008).

[41] National Instrument board

[42] MATLAB’s findpeaks algorithm